Hindawi
Wireless Communications and Mobile Computing
Volume 2021, Article ID 5537517, 10 pages
https://doi.org/10.1155/2021/5537517

Research Article

Joint Position and Time Allocation Optimization of UAV-Aided Wireless Powered Relay Communication Systems

Xiaofei Di[1] **and Yang Chen**[2]

[1]*School of Software Engineering, Beijing Jiaotong University, Beijing 100044, China*
[2]*School of Communication Engineering, Hangzhou Dianzi University, Hangzhou 310018, China*

Correspondence should be addressed to Xiaofei Di; xfdi@bjtu.edu.cn

Received 25 February 2021; Revised 26 March 2021; Accepted 7 April 2021; Published 19 April 2021

Academic Editor: Dung Le

The Internet of things (IoT) has emerged as a platform for connecting massive physical devices to collect and analyze data for decision-making. Wireless devices in IoT are usually energy-constrained and thus need to be powered by a stable and reliable energy source in order to maintain a long network lifetime. An unmanned aerial vehicle (UAV) as an energy source is a proper and applicable way to supply energy to wireless devices in IoT, due to its flexibility and potential of providing line-of-sight (LOS) links for wireless air-to-ground channels. In this paper, a UAV-aided wireless powered relay communication system is presented, where a UAV firstly emits energy to a source and a relay, and then, the source and relay cooperatively transmit information to their destination. To explore the performance limit of the system, a problem is formulated by jointly optimizing the position of the UAV and time allocation to maximize the achievable information rate of the system. By deriving the explicit expressions of the optimal position of UAV and optimal time fraction, the nonconvex optimization problem is efficiently solved. Simulation results show that our proposed method significantly outperforms the benchmark methods.

1. Introduction

With the development of the fifth generation (5G) mobile networks, including machine-type communications (MTC), the Internet of things (IoT) has gradually become reality [1, 2]. In typical applications of IoT, a large number of sensors collect and transmit information to the sink node, and then, the sink node processes the received information to assist analysis and decision. Sensors in IoT generally need to work for 10 to 15 years [3]. However, they are usually energy-constrained nodes, so it is very important to supply sensors with stable and reliable energy in order to prolong the lifetime of IoT. Conventionally replacing batteries of the sensors is inconvenient for the massive sensors usually sparsely distributed in a wide area.

The wireless power transfer (WPT) technology provides a feasible way to satisfy the requirement of energy supply of sensors in IoT, where sensors are powered by radio frequency (RF) energy transfer [4]. Recently, a wireless powered communication network (WPCN) has emerged as a promising technique by combining WPT and communication technologies. In WPCN, energy-constrained sensors have to complete information transmissions by using the energy harvested from a dedicated power beacon (PB) [5] or a hybrid access point (H-AP) [6]. In [5], a dedicated PB was deployed to supply energy to two communication nodes, and then, the two communication nodes exchanged information by using their harvested energies. In [6], a H-AP firstly transferred energy to multiple users and then received the information which the users transmitted by using the harvested energy. In [7], WPCN was combined with a relay technique, where a source and a relay harvested energy from a signal emitted by a PB, then cooperatively transmitted information to a destination. However, in the existing works, PB or H-AP is fixed at a position; it is difficult to satisfy energy supply requirements of a massive number of sensors in IoT. On the one hand, due to widely and sparsely distributed sensors, a lot of fixed PBs or HAPs have to be applied, which

significantly increases the deployment cost. On the other hand, fixed PBs or HAPs are hard to apply in some special environments such as toxic or remote forest regions.

Recently, unmanned aerial vehicle- (UAV-) aided WPCNs have attracted considerable attention, where UAV acts as an aerial PB or HAP to help energy and information transmission. Due to the inherent flexibility and mobility, UAV-aided WPCNs can efficiently solve the problems of fixed PBs or HAPs mentioned above. Moreover, UAV has potential to provide line-of-sight (LOS) links for wireless air-to-ground channels, so it can significantly enhance the energy transfer or communication performance [8]. According to [9], UAVs can be classified into two types, that is, mobile UAVs and static UAVs. The two types of UAVs have different advantages and applications, so both of them have attracted much interest.

Mobile UAV-aided WPCNs were studied in [10–13]. In [10, 11], a mobile UAV-aided multiuser WPCN was studied, where a mobile UAV first wirelessly charged multiple users on the ground and then received the information from the users, and the packet loss rate and energy consumption of the UAV performance were minimized, respectively. In [12], two UAVs wirelessly charged two users on the ground and collected information from them, respectively. For the two-UAV two-user interference channel, the common throughput of two uses was maximized. [13] further investigated multiple UAV multiple user scenarios and minimized the communication delay. Mobile UAVs are not capable of hovering, which limits the power transfer efficiency. Moreover, mobile UAV-aided WPCNs involve the optimization of continuous functions on trajectory, and its complexity is high [11–13]. So, mobile UAVs must be equipped with large computation capacity to satisfy the requirement of optimization algorithms.

In this paper, we consider static UAV communication systems, where static UAVs can hover over a fixed position by equipping propellers on UAVs [14–16]. Recently, static UAVs have been considered to apply to WPCNs. Compared with mobile UAVs, static UAVs can supply more stable and reliable services due to their hovering. Moreover, static UAV-aided WPCNs only need to design the hovering positions of UAVs, which simplifies the system design, and therefore can deploy UAVs without large computation capacity in networks. In addition, static UAVs can also be realized by the tethered UAVs, which are connected by a cable/wire with a ground control platform to satisfy their requirement of energy supply, such as AT&T's flying cell-on-wings (COWs) and Facebook's Tether-Tenna [17].

Due to the reasons above, static UAV-aided WPCNs have also attracted research interest [18–21]. In [18], a static UAV acting as H-AP firstly emitted energy to multiple users and then received the information from the users, and the performance of throughput was investigated and optimized by jointly optimizing UAV position and time allocation. In [19], a UAV-aided WPCN was investigated, where a UAV as relay firstly simultaneously received energy and information from the signal transmitted by a source and then helped to forward received information to a destination by using the harvested energy. The outage performance of the system was analyzed. This way is referred to as simultaneous wireless information and power transfer (SWIPT) [22]. The authors in [20] considered the identical system model with [19] and further minimized the outage probability by jointly optimizing UAV position and system parameters. [21] extended [19] to a multiple destination scenario and reduced UAV's energy consumption by optimizing the UAV position.

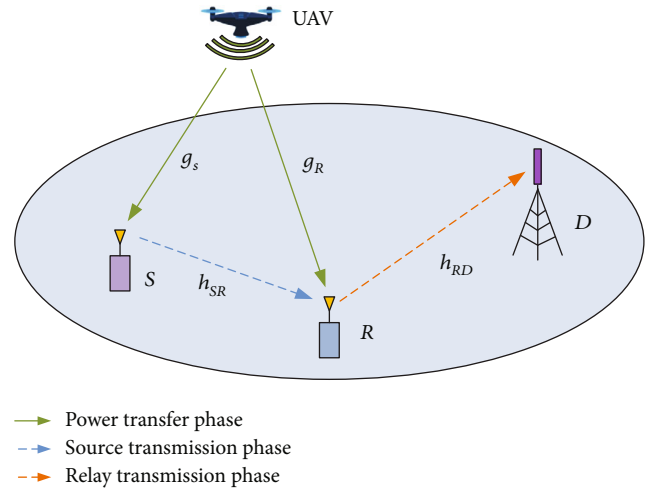

Figure 1: UAV-aided wireless powered relay communication network.

Different from the existing works mentioned above, in this paper, we consider a static UAV-aided wireless powered relay communication system, where a static UAV serves as a PB to provide energy to a source and a relay, and then, the source and relay cooperatively transmit information to their destination, as shown in Figure 1. As a practical application of the presented system in IoT, the source and relay are energy-constrained sensors, and the destination is a sink node with a fixed energy source. They cannot directly communicate due to long distances between sensors and sink, so sensors have to cooperatively transmit information by the relaying way. Moreover, the sensors may be located in a toxic environment, and therefore, UAV is a better way to transfer power to the energy-constrained sensors. To explore the performance limit of the system, a problem is formulated by jointly optimizing the position of the UAV and time allocation to maximize the achievable information rate of the system.

Our contributions are summarized as follows. Firstly, we propose a UAV-aided wireless powered relay communication system, which reduces the deployment cost thanks to the flexibility of UAV, compared with fixed PB. Secondly, due to the coupling of optimized variables, the optimization problem is nonconvex. To this end, we decompose the problem into two subproblems to, respectively, derive the explicit expressions of the optimal position of UAV and optimal time allocation. Thirdly, simulation results show that our proposed method is significantly superior to the benchmark methods. Finally, the effect of relay position on the system is demonstrated, and it provides some insights for future application of the UAV-aided wireless powered relay communication system.

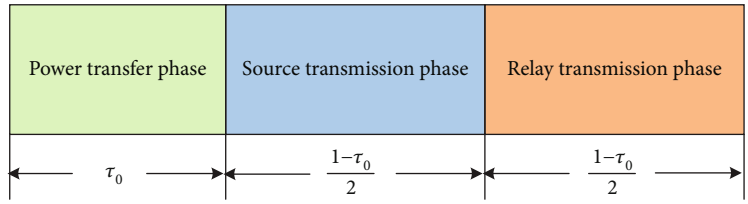

Figure 2: The transmission procedure.

The rest of this paper is organized as follows. In Section 2, the system model is given and an optimization problem is formulated. Section 3 proposes an efficient method to solve the optimization problem. Section 4 gives simulation results to illustrate the system performance. Finally, Section 5 concludes this paper.

2. System Model

We consider a UAV-aided wireless powered relay communication network consisting of a source (S), a relay (R), and a destination (D) on the ground, as well as a UAV (U) in the air, as shown in Figure 1. The source wishes to transmit the information to the destination with the assistance of the half-duplex decode-and-forward (DF) relay. It is assumed that the direct link from the source to the destination does not exist. The source and relay are energy-constrained nodes, and thus, they have to harvest energy from the signal emitted by the UAV. All the nodes of the network are deployed with a single antenna.

A three-dimensional (3D) Cartesian coordinate system is considered, since there simultaneously exist air-to-ground (ATG) channels, i.e., the channels from the UAV to the nodes on the ground (S, R), and ground-to-ground (GTG) channels, i.e., the channel from S to R and that from R to D . The UAV is assumed to hover at a fixed altitude H, and its position is denoted as $d_U = (x_U, y_U, H)$. The positions of the nodes on the ground are denoted as $d_v = (x_v, y_v, 0), v \in \{S, R, D\}$.

According to the preliminary channel measurement results, the ATG channels typically consist of strong LoS links [23]. Further, according to 3GPP, when the altitude of UAV exceeds 40 m [24], the LOS probability is 100% in a rural environment. Therefore, in this paper, the channel power gain from the UAV to S and R is, respectively, modeled as

$$g_v = \frac{\beta_A}{\|dU - d_v\|^{\alpha_A}}, \quad v \in \{S, R\}, \tag{1}$$

where α_A and β_A represent the path loss factor and the channel power gain at unit reference distance for the ATG channel, respectively. For the GTG channel, the channel power gain between two nodes is modeled as

$$h_{uv} = \frac{\beta_G \rho^2}{\|d_u - d_v\|^{\alpha_G}}, \quad u \in \{S, R\}, v \in \{R, D\}, \tag{2}$$

where ρ^2 is a random variable following exponential distribution with unit mean. α_G and β_G represent the path loss factor and the channel power gain at unit reference distance for the GTG channel, respectively.

The transmission procedure is divided into three phases, that is, the power transfer (PT) phase, source transmission (ST) phase, and relay transmission (RT) phase, as shown in Figure 2. The duration of each transmission procedure is denoted as T. In the first phase of duration $\tau_0 T (0 < \tau_0 < 1)$, i.e., the PT phase, the UAV emits the energy to the source and the relay. The signal received by the source and the relay can be, respectively, given as

$$e_v = \sqrt{g_v P} x_0 + n_v, \quad v \in \{S, R\}, \tag{3}$$

where P is the transmit power of UAV, x_0 is the signal of unit energy transmitted by UAV, and n_v is the additive white Gaussian noise (AWGN) with power σ^2.

Thus, in the PT phase, the energy harvested by S and R can be expressed as

$$E_v = \eta \tau_0 T g_v P, \quad v \in \{S, R\}, \tag{4}$$

where η is the energy harvesting efficiency and satisfies $0 \le \eta \le 1$.

In the second phase of duration $(1 - \tau_0)T/2$, i.e., ST phase, S transmits information to R, and the signal received by R can be expressed as

$$y_R = \sqrt{h_{SR} P_S} x_S + n_R, \tag{5}$$

where n_R is AWGN with power σ^2 and $P_S = E_S/(1 - \tau_0)T/2$ is the transmit power of S. By using (1) and (4), P_S can be further calculated as

$$P_S = \frac{2\eta \tau_0 \beta_A P}{(1 - \tau_0)\|d_U - d_S\|^{\alpha_A}}. \tag{6}$$

From (5), the received signal-to-noise ratio (SNR) at R can be calculated as

$$\gamma_R = \frac{h_{SR} P_S}{\sigma^2}. \tag{7}$$

By using (6), (7) can be transformed into

$$\gamma_R = \frac{2\tau_0}{1-\tau_0}\frac{L_1}{\|d_U - d_S\|^{\alpha_A}}, \tag{8}$$

where $L_1 = \eta\beta_A h_{SR} P/\sigma^2$.

Therefore, the achievable information rate from S to R can be expressed as

$$\mathscr{R}_{SR} = \frac{1-\tau_0}{2}\log_2(1+\gamma_R). \tag{9}$$

In the third phase of duration $(1-\tau_0)T/2$, i.e., RT phase, R first decodes the information and then forwards decoded information to D, and the signal received by D can be expressed as

$$y_D = \sqrt{h_{RD}P_R}x_R + n_D, \tag{10}$$

where n_D is AWGN with power σ^2 and $P_R = E_R/(1-\tau_0)T/2$ is the transmit power of R. By using (1) and (4), P_R can be expressed as

$$P_R = \frac{2\eta\tau_0\beta_A P}{(1-\tau_0)\|d_U - d_R\|^{\alpha_A}}. \tag{11}$$

From (10) and (11), the received SNR at D can be calculated as

$$\gamma_D = \frac{h_{RD}P_R}{\sigma^2} = \frac{2\tau_0}{1-\tau_0}\frac{L_2}{\|d_U - d_R\|^{\alpha_A}}, \tag{12}$$

where $L_2 = \eta\beta_A h_{RD} P/\sigma^2$, and therefore, the achievable information rate from R to D can be expressed as

$$\mathscr{R}_{RD} = \frac{1-\tau_0}{2}\log_2(1+\gamma_D). \tag{13}$$

The end-to-end achievable information rate of the system is the minimum of $\mathscr{R}_{SR}$ and $\mathscr{R}_{RD}$, that is,

$$\mathscr{R} = \frac{1-\tau_0}{2}\log_2\left(1+\frac{2\tau_0}{1-\tau_0}\min\left\{\frac{L_1}{\|d_U - d_S\|^{\alpha_A}}, \frac{L_2}{\|d_U - d_R\|^{\alpha_A}}\right\}\right). \tag{14}$$

Our objective is to maximize the end-to-end achievable information rate $\mathscr{R}$ by jointly optimizing the position of UAV and time allocation, and therefore, the corresponding optimal problem is formulated as

$$\begin{aligned} \mathbf{P1}: &\max_{\tau_0, x_U, y_U} \mathscr{R}, \\ &\text{s.t.} 0 < \tau_0 < 1. \end{aligned} \tag{15}$$

3. Problem Solution

The optimization problem **P1** is a nonconvex problem, due to the coupling of optimized variables. In this section, problem **P1** is first transformed into an equivalent problem, and then, it is efficiently solved by our proposed algorithm.

3.1. Equivalent Problem of Problem **P1**. In this subsection, the original problem **P1** is transformed into an equivalent problem, and the result is given in Proposition 2 as follows.

Algorithm 1. Algorithm of solving problem **P1**.

(1) Obtain the optimal UAV position (x_U^*, y_U^*, H) and the optimal value d^* by solving problem **P3**

(2) Obtain the optimal τ_0^* by solving problem **P2** with the obtained d^*

(3) Calculate the optimal value of problem **P1** by using the obtained x_U^*, y_U^* and τ_0^*

Proposition 2. *Problem **P1** is equivalent to the following problem **P2**:*

$$\mathbf{P2}: \max_{\tau_0} \frac{1-\tau_0}{2}\log_2\left(1+\frac{2\tau_0}{1-\tau_0}d^*\right), \tag{16}$$

$$s.t. 0 < \tau_0 < 1, \tag{17}$$

*where d^* is the optimal value of the following problem **P3**:*

$$\mathbf{P3}: d^* = \max_{x_U, y_U} \min\left\{\frac{L_1}{\|d_U - d_S\|^{\alpha_A}}, \frac{L_2}{\|d_U - d_R\|^{\alpha_A}}\right\}. \tag{18}$$

Proof. Proposition 2 can be proved by the similar method adopted in [7], and thus, the proof is omitted here.

By using Proposition 2, the original problem **P1** can be decomposed into two successive subproblems **P3** and **P2** to solve. Firstly, by solving problem **P3**, the optimal UAV position is obtained. Then, by substituting the obtained optimal value d^* of **P3** into (16) and solving problem **P2**, the optimal time allocation is obtained. Finally, by using obtained optimal UAV position and time allocation, the maximal achievable information rate can be calculated. Algorithm 1 gives the detailed procedure.

In the rest of this section, problem **P3** and **P2** are dealt with sequentially to obtain their explicit optimal solution.

3.2. Solution of Problem **P3**. From problem **P3**, it can be observed that the solution of the problem depends on the distances from UAV to S (i.e., U-S) and from UAV to R (i.e., U-R). Without loss of generality, the considered coordinate system is set as shown in Figure 3. S is placed at the origin with coordinate (0, 0, 0). R is located at the positive axis of the X-axis, and its coordinate is $(x_R, 0, 0)$, where $x_R > 0$. D is located on the X-Y plane, and its coordinate is $(x_D, y_D, 0)$. It is worth noting if system nodes are in a practical geographical coordinate system; it can be changed to our consider coordinate system by translation and rotation transformations [25]. Figure 3 plots two possible positions of UAV, i.e., a general position $U_1(x_U, y_U, H)$ and a special position

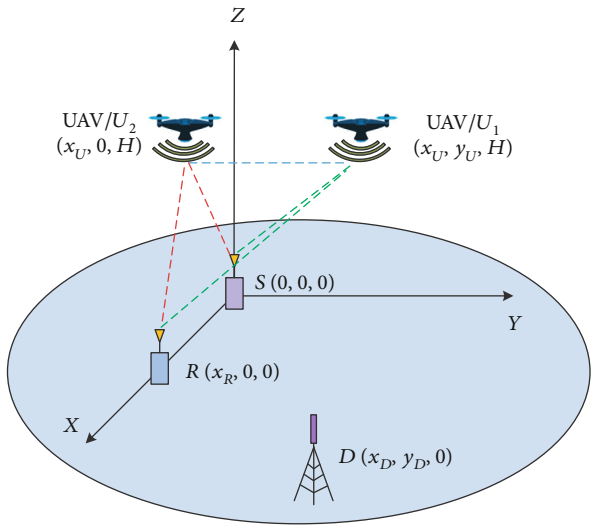

FIGURE 3: The considered 3D coordinate system.

$U_2(x_U, 0, H)$. We can prove the following lemma, which shows that the position U_1 is superior to U_2.

Lemma 3. *There exists a position (x_U, y_U, H) of UAV satisfying the following condition, which can achieve the optimum of problem **P3**:*

$$\begin{cases} 0 \le x_U \le x_R, \\ y_U = 0. \end{cases} \tag{19}$$

Proof. Firstly, we prove that at the optimum of problem **P3**, $y_U = 0$. That is, in Figure 3, the position of U_2 is superior to U_1. Observing problem **P3**, it can be found that the solution of the problem depends on the distances of U-S and U-R, and less distances lead to a greater objective function. According to the geometrical relations, one can easily see that the distance from U_2 to S is less than that from U_1 to S. Similarly, the distance from U_2 to R is less than that from U_1 to R. So, at the optimum, $y_U = 0$.

Secondly, we prove that there exists a position $(x_U, 0, H)$ of UAV satisfying (19), which can achieve the optimum of problem **P3**. Figure 4 plots two possible positions of UAV, i.e., $U_1(x_U^{(1)}, 0, H)$ satisfying (19) and $U_2(x_U^{(2)}, 0, H)$ not satisfying (19). It is noting that for the cases not satisfying (19), we only consider the case $x_U^{(2)} < 0$, and the other case $x_U^{(2)} > x_R$ is neglected, due to the symmetry.

Further, we divide $x_U^{(2)} < 0$ into the following two intervals to discuss. On the one hand, when $x_U^{(2)} < -x_U^{(1)}$, it can be easily seen that the distance of U_2-S is greater than that of U_1-S and the distance of U_2-R is greater than that of U_1-R. This means that for problem **P3**, the position of U_1 is superior to U_2. On the other hand, when $-x_U^{(1)} \le x_U^{(2)} \le 0$, we can adjust the position of U_1 in order so that $x_U^{(1)} = -x_U^{(2)}$. At this moment, the distance of U_2-S is equal to that of U_1-S, and the distance of U_2-R is greater than or equal to that of U_1-R. Therefore, the first term of the objective function of problem **P3** with position U_1 is equal to that with U_2 while the second term of the objective function of problem **P3** with U_1 is larger than that with U_2. This means that for problem **P3**, when UAV is located at U_1, it makes the objective function of problem **P3** either become larger than U_2 or be equal to U_2. So, this lemma is proved.

Lemma 3 shows that the UAV should be deployed at some position with height H above the line between S and R. In the following, we derive the optimal X-axis cordinate x_U of the UAV.

Using Lemma 3, problem **P3** can be transformed into the following problem **P4**:

$$\mathbf{P4}: d^* = \max_{x_U} \min \left\{ \frac{L_1}{\left(x_U^2 + H^2\right)^{\alpha_A/2}}, \frac{L_2}{\left[\left(x_U - x_R\right)^2 + H^2\right]^{\alpha_A/2}} \right\}, \quad \text{s.t.} 0 \le x_U \le x_R. \tag{20}$$

For problem **P4**, the following proposition can be derived.

Proposition 4. *The optimal x_U^* of problem **P4** is given by*

$$x_U^* = \begin{cases} 0, & \text{if } L > 1 \text{ and } x_R < H\sqrt{L-1}, \\ x_R, & \text{if } L < 1 \text{ and } x_R < H\sqrt{\left(\frac{1}{L} - 1\right)}, \\ \frac{x_R}{2}, & \text{if } L = 1, \\ \kappa, & \text{else}, \end{cases} \tag{21}$$

where $\kappa = \sqrt{Lx_R^2 - (L-1)^2 H^2} - x_R/(L-1)$ *and* $L = (L_2/L_1)^{2/\alpha_A}$.

Proof. Let $T_1(x_U) = L_1/(x_U^2 + H^2)^{\alpha_A/2}$ and $T_2(x_U) = L_2/[(x_U - x_R)^2 + H^2]^{\alpha_A/2}$. It can be easily found that when $0 \le x_U \le x_R$, T_1 is a decreasing function of x_U while T_2 is an increasing function of x_U. Figure 5 plots all the possible cases of two functions $T_1(x_U)$ and $T_2(x_U)$.

For Figure 5(a), this case happens when $T_1(0) < T_2(0)$, i.e., $L > 1$ and $x_R < H\sqrt{L-1}$. For this case, we can have the optimal $x_U^* = 0$ and the corresponding $d^* = L_1/H^{\alpha_A}$.

For Figure 5(b), this case happens when $T_1(x_R) > T_2(x_R)$, i.e., $L < 1$ and $x_R < H\sqrt{(1/L - 1)}$. For this case, we can have the optimal $x_U^* = x_R$ and the corresponding $d^* = L_2/H^{\alpha_A}$.

For the remaining Figures 5(c) and 5(d), problem **P4** achieves the optimum, when

$$T_1(x_U) = T_2(x_U). \tag{22}$$

After some simple algebraic manipulations, (22) is transformed into

$$(L-1)x_U^2 + 2x_R x_U + (L-1)H^2 - x_R^* = 0. \tag{23}$$

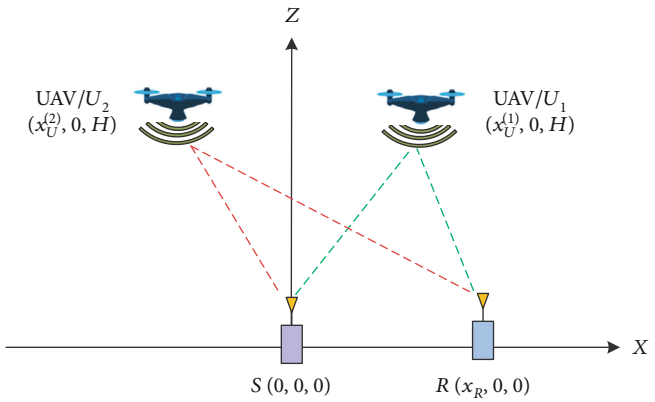

FIGURE 4: The X-Z plane of the considered 3D coordinate system.

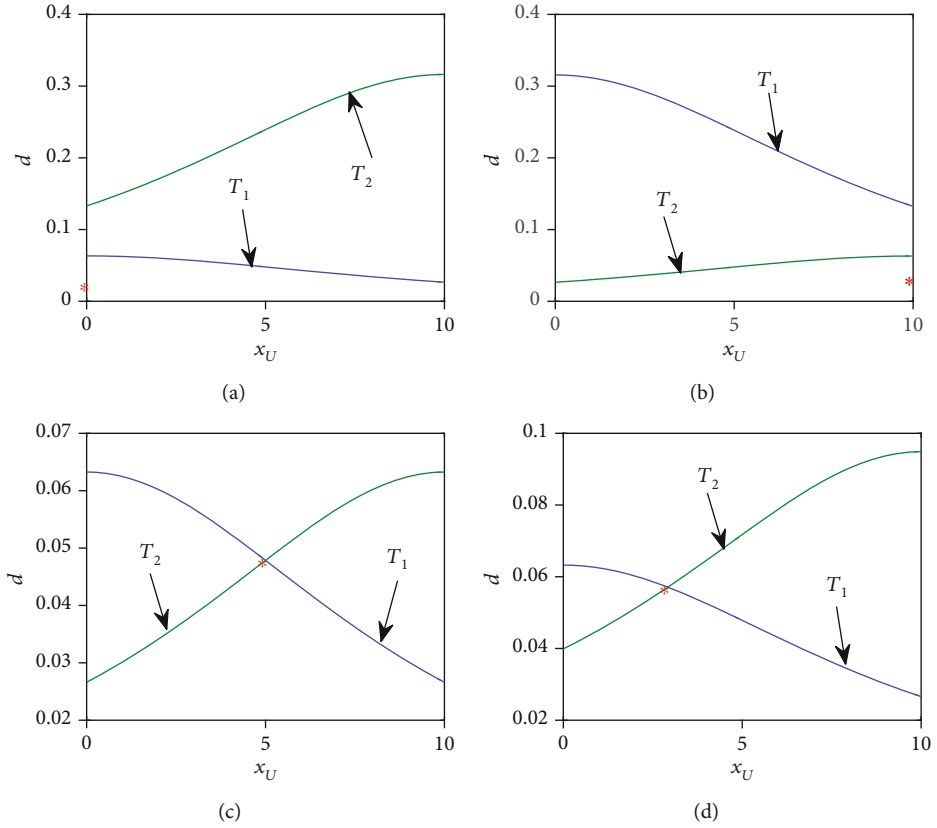

FIGURE 5: The four cases for function $T_1(x_U)$ and $T_2(x_U)$. The red $(*)$ represents the optimal point of problem **P4**.

If $L = 1$, corresponding to Figure 5(c), (23) becomes $2x_R x_U - x_R^* = 0$, and thus, $x_U^* = x_R/2$.

Otherwise, corresponding to Figure 5(d), (23) is a quadratic equation of x_U, and we can obtain the root of this equation as

$$x_U^* = \frac{\sqrt{Lx_R^* - (L-1)^2 H^2} - x_R}{L-1}. \tag{24}$$

Substituting the obtained x_U^* into $T_1(x_U)$ or $T_2(x_U)$, the corresponding d^* can be calculated. Thus, this proposition is proved.

Lemma 3 and Proposition 4 show that to achieve the best system performance, the UAV should be placed at the position above the line between S and R, where its height is H and horizontal distance away from S is $x^* U$.

3.3. Solution of Problem **P2**. For problem **P2**, we can derive the following proposition to obtain the optimal solution.

Proposition 5. *The optimal τ_0^* of problem **P2** is given by*

$$\tau_0^* = \frac{e^{W_0((2d^*-1)/e)+1} - 1}{e^{W_0((2d^*-1)/e)+1} + 2d^* - 1}, \tag{25}$$

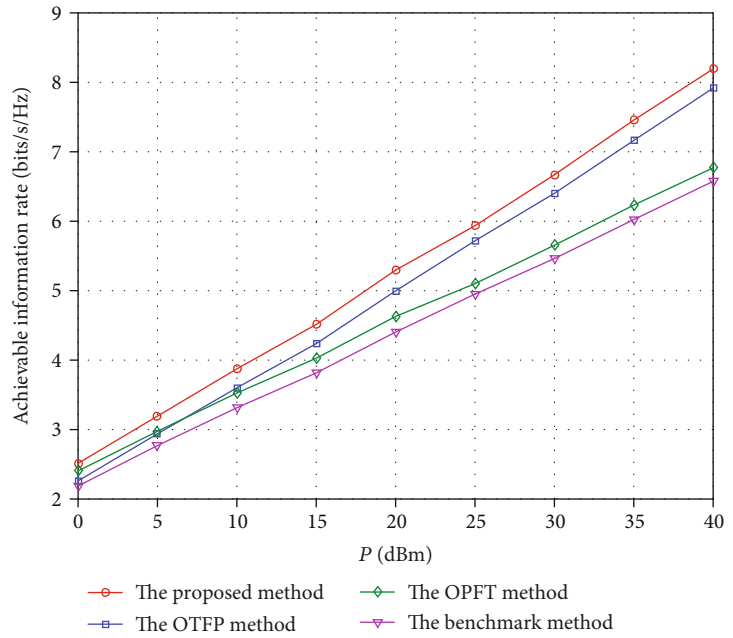

Figure 6: Performance comparisons of the proposed method and three other methods.

where $W_0(x)$ is the branch satisfying $W(x) \geq -1$ of Lambert W function $W(x)$ [26].

Proof. The objective function of problem **P2** is concave due to its second derivative $-2(d^*)^2/(1-\tau_0+2\tau_0 d^*)^2(1-\tau_0)\ln(2) \leq 0$. To obtain the maximal value of the objective function, let its first derivative be equal to zero, so we have

$$\left(1+\frac{2d^*\tau_0}{1-\tau_0}\right)\ln\left(1+\frac{2d^*\tau_0}{1-\tau_0}\right)=2d^*+\frac{2d^*\tau_0}{1-\tau_0}. \tag{26}$$

Let

$$1+\frac{2d^*\tau_0}{1-\tau_0}=y, \tag{27}$$

and we can easily obtain that $y > 1$, due to $d^* > 0$ and $0 < \tau_0 < 1$. After some simple algebraic manipulations for (26), we can have

$$y\ln y = y + 2d^* - 1. \tag{28}$$

(28) can be further transformed into

$$\ln\left(\frac{y}{e}\right)e^{\ln(y/e)}=\frac{2d^*-1}{e}. \tag{29}$$

According to the definition of the Lambert W function, we can have

$$\ln\left(\frac{y}{e}\right)=W\left(\frac{2d^*-1}{e}\right). \tag{30}$$

Then, we can have

$$y = e^{W((2d^*-1)/e)+1}. \tag{31}$$

According to the obtained condition $y > 1$, we can have $W((2d^*-1)/e) > -1$. This means that the $W_0(x)$ branch is adopted in (31). Then, after some simple algebraic manipulations for (27), we can obtain

$$\tau_0^* = \frac{e^{W_0(2d^*-1/e)+1}-1}{e^{W_0((2d^*-1)/e)+1}+2d^*-1}. \tag{32}$$

This proposition is thus proved.

Finally, we analyze the computation complexity of Algorithm 1. Algorithm 1 is composed of three successive steps. In the first step and the second step, the explicit expressions of the optimal UAV position and optimal time fraction are, respectively, used, and thus, the complexity is $O(1)$. By using the obtained optimal UAV position and time fraction, the optimal value can be calculated by using (14), and thus, its complexity is also $O(1)$. So, the total complexity of Algorithm 1 is $O(1)$.

4. Simulation Results

This section gives simulation results to illustrate the performance of the presented system and proposed algorithm. In the simulations, the considered 3D coordinate system is shown in Figure 3, where S is located at (0, 0, 0), R is at (0, 100, 0), and D is at (200, 200, 0). The UAV is set to hover at the altitude of $H = 50$ m. The noise power is $\sigma^2 = -130$ dBm. According to [5], the path loss factor α_A and the channel power gain β_A at unit reference distance for the ATG channel are set to be $\alpha_A = 2$ and $\beta_A = 30$ dB, respectively. The path loss factor α_G and the

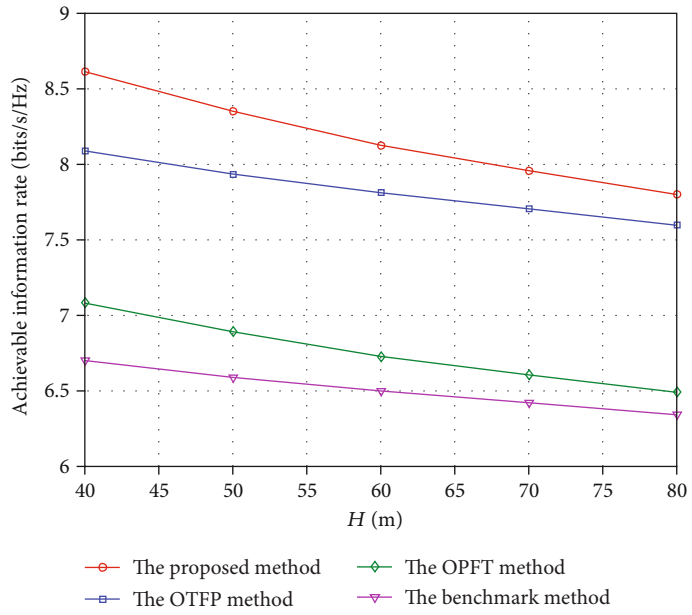

Figure 7: The effect of UAV altitude on achievable information rate performance.

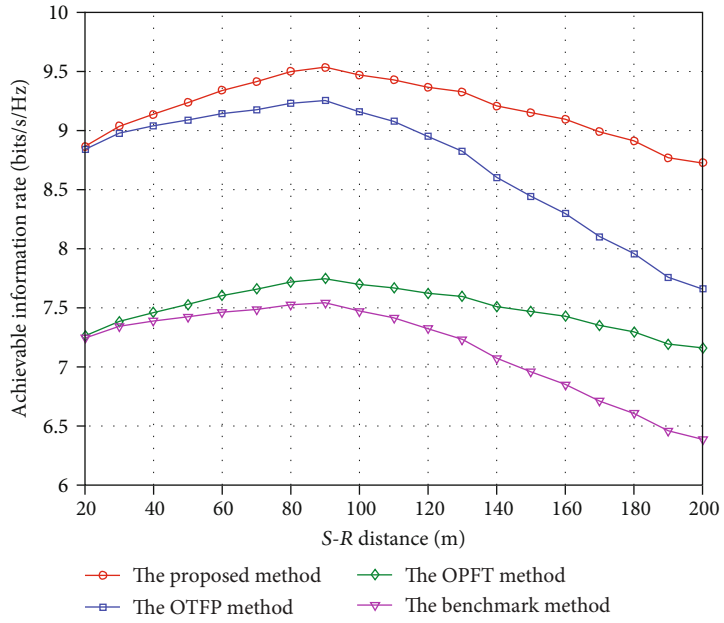

Figure 8: The effect of relay position on achievable information rate performance.

channel power gain β_G at unit reference distance for the GTG channel are set to be $\alpha_G = 3$ and $\beta_G = -30$ dB, respectively. The energy harvesting efficiency η is set to 1 in order to explore the performance limit of the system.

4.1. Performance Comparisons. In this subsection, the performance of the proposed method is compared with three other methods, i.e., (1) The benchmark method: fixed time fraction $\tau_0 = 1/3$ and fixed position of UAV $d_U = (50, 0, 50)$; that is, UAV hovers above the middle point between S and R; (2) The optimal time fraction and fixed position (OTFP) method: fixed position of UAV $d_U = (50, 0, 50)$ and optimal time fraction τ which is set according to (25); (3) The optimal position and fixed time fraction (OPFT) method: fixed time fraction $\tau_0 = 1/3$ and the optimal position of UAV which is set according to (21). Figure 6 shows the achievable information rates of the proposed method and three other methods with respect to the power of UAV P. It can be found that the achievable information of the proposed method is significantly superior to the three other methods.

4.2. The Effect of UAV Altitude on System Performance. In this subsection, the effect of UAV altitude on the achievable information rate of the system is demonstrated in Figure 7,

where the power of UAV is set to be $P = 40$ dBm. One can observe that with the increase of the altitude of UAV, the achievable information rates of the four methods decrease. Moreover, our proposed method outperforms the three other methods, which agrees with Figure 6. It can also be found that the achievable information rate of the proposed method is reduced faster than the OTFP one as the UAV altitude increases. The reason may be as follows. From (14), it can be seen that the optimal UAV position helps to reduce the distances from UAV to S and from UAV to R, and thus, the transmit power of S and R can be significantly increased. This further leads to very higher SNR, which is a more key factor for the achievable information rate of the system compared with time allocation. As the UAV altitude increases, the distance from UAV to S and that from UAV to R will be dominated by the altitude of UAV, and therefore, the gap of the two methods will gradually decrease.

4.3. The Effect of Relay Position on System Performance. In this subsection, we discuss the effect of relay position on the achievable information rate of the system. The UAV is set to hover at the altitude of $H = 50$ m. S is set to be located at (0, 0, 0), and D is at (200, 0, 0), which means that both S and D are located at the X-axis. The relay is also set to be located at the X-axis, and its position is denoted by the distance from S to R (i.e., S-R). The power of UAV is set to be $P = 40$ dBm. Figure 8 shows the achievable information rates of the four methods with respect to the distance of $S - R$. It can be seen that with the increase of S-R distance, the achievable information rate of the system firstly increases and then gradually decreases. Moreover, when R is at the position of about 90 m away from S, the system performance achieves the maximum.

5. Conclusions

In this paper, a UAV-aided wireless powered relay communication system has been presented, where a UAV firstly supplies energy to a source and a relay, and then, the source and relay cooperatively transmit information to their destination. An efficient algorithm has been proposed to maximize the achievable information rate of the system by deriving the explicit expressions of the optimal position of UAV and optimal time fraction. Simulation results have shown that our proposed algorithm significantly outperforms the benchmark methods. The effect of relay position on the system has also been demonstrated, which provides some insights for the deployment of relay in UAV-aided wireless powered relay communication systems in IoT.

Data Availability

The data used to support the findings of this study are available from the corresponding author upon request.

Conflicts of Interest

The authors declare that they have no conflicts of interest.

Acknowledgments

This work was supported by the National Natural Science Foundation of China under Grant (no. 61801155), by the Natural Science Foundation of Zhejiang Province (no. LQ20F040001), and by the Opening Project of Beijing Key Lab of Traffic Data Analysis and Mining (Research on Mobile Edge Computing-based Cooperative Computing Mechanism for Vehicular Networks).

References

[1] L. Chettri and R. Bera, "A comprehensive survey on internet of things (IoT) toward 5G wireless systems," *IEEE Internet of Things Journal*, vol. 7, no. 1, pp. 16–32, 2020.

[2] P. X. Nguyen, D. H. Tran, O. Onireti et al., "Backscatter-assisted data offloading in OFDMA-based wireless powered mobile edge computing for IoT networks," *IEEE Internet of Things Journal*, 2021.

[3] M. Webb, "3GPP's low-power wide-area IoT solutions: NB-IoT and eMTC, RWS-180023," in *Workshop on 3GPP Submission Towards IMT-2020*, Brussels, Belgium, 2018.

[4] K. W. Choi, L. Ginting, P. A. Rosyady, A. A. Aziz, and D. I. Kim, "Wireless-powered sensor networks: how to realize," *IEEE Transactions on Wireless Communications*, vol. 16, no. 1, pp. 221–234, 2017.

[5] C. Zhong, H. Liang, H. Lin, H. A. Suraweera, F. Qu, and Z. Zhang, "Energy beamformer and time split design for wireless powered two-way relaying systems," *IEEE Transactions on Wireless Communications*, vol. 17, no. 6, pp. 3723–3736, 2018.

[6] H. Ju and R. Zhang, "Throughput maximization in wireless powered communication networks," *IEEE Transactions on Wireless Communications*, vol. 13, no. 1, pp. 418–428, 2014.

[7] C. Zhong, G. Zheng, Z. Zhang, and G. K. Karagiannidis, "Optimum wirelessly powered relaying," *IEEE Signal Processing Letters*, vol. 22, no. 10, pp. 1728–1732, 2015.

[8] D.-H. Tran, T. X. Vu, S. Chatzinotas, S. ShahbazPanahi, and B. Ottersten, "Coarse trajectory design for energy minimization in UAV-enabled," *IEEE Transactions on Vehicular Technology*, vol. 69, no. 9, pp. 9483–9496, 2020.

[9] M. Mozaffari, W. Saad, M. Bennis, and M. Debbah, "Unmanned aerial vehicle with underlaid device-to-device communications: performance and tradeoffs," *IEEE Transactions on Wireless Communications*, vol. 15, no. 6, pp. 3949–3963, 2016.

[10] K. Li, W. Ni, B. Wei, and E. Tovar, "Onboard double Q-learning for airborne data capture in wireless powered IoT networks," *IEEE Networking Letters*, vol. 2, no. 2, pp. 71–75, 2020.

[11] Z. Yang, W. Xu, and M. Shikh-Bahaei, "Energy efficient UAV communication with energy harvesting," *IEEE Transactions on Vehicular Technology*, vol. 69, no. 2, pp. 1913–1927, 2020.

[12] L. Xie, J. Xu, and Y. Zeng, "Common throughput maximization for UAV-enabled interference channel with wireless powered communications," *IEEE Transactions on Communications*, vol. 68, no. 5, pp. 3197–3212, 2020.

[13] P. Wu, F. Xiao, H. Huang, and R. Wang, "Load balance and trajectory design in Multi-UAV aided large-scale wireless rechargeable networks," *IEEE Transactions on Vehicular Technology*, vol. 69, no. 11, pp. 13756–13767, 2020.

[14] J. Lyu, Y. Zeng, R. Zhang, and T. J. Lim, "Placement optimization of UAV-mounted mobile base stations," *IEEE Communications Letters*, vol. 21, no. 3, pp. 604–607, 2017.

[15] S. Fu, Y. Tang, N. Zhang, L. Zhao, S. Wu, and X. Jian, "Joint unmanned aerial vehicle (UAV) deployment and power control for internet of things networks," *IEEE Transactions on Vehicular Technology*, vol. 69, no. 4, pp. 4367–4378, 2020.

[16] L. Li, T.-H. Chang, and S. Cai, "UAV positioning and power control for two-way wireless relaying," *IEEE Transactions on Wireless Communications*, vol. 19, no. 2, pp. 1008–1024, 2020.

[17] Q. Wu, J. Xu, and R. Zhang, "Capacity characterization of UAV-enabled two-user broadcast channel," *IEEE Journal on Selected Areas in Communications*, vol. 36, no. 9, pp. 1955–1971, 2018.

[18] M. Jiang, Y. Li, Q. Zhang, and J. Qin, "Joint position and time allocation optimization of UAV enabled time allocation optimization networks," *IEEE Transactions on Communications*, vol. 67, no. 5, pp. 3806–3816, 2019.

[19] L. Yang, J. Chen, M. O. Hasna, and H. C. Yang, "Outage performance of UAV-assisted relaying systems with RF energy harvesting," *IEEE Communications Letters*, vol. 22, no. 12, pp. 2471–2474, 2018.

[20] Y. H. Kim, I. A. Chowdhury, and I. Song, "Design and analysis of UAV-assisted relaying with simultaneous wireless information and power transfer," *IEEE Access*, vol. 8, pp. 27874–27886, 2020.

[21] S. Chen, X. Li, C. Luo, H. Ji, and H. Zhang, "Energy-efficient power, position and time control in UAV-assisted wireless networks," in *Proc. IEEE Globecom Workshops*, pp. 1–6, Waikoloa, HI, USA, Decemeber 2019.

[22] X. Di, K. Xiong, P. Fan, and H.-C. Yang, "Simultaneous wireless information and power transfer in cooperative relay networks with rateless codes," *IEEE Transactions on Vehicular Technology*, vol. 66, no. 4, pp. 2981–2996, 2017.

[23] D. W. Matolak and R. Sun, "Unmanned aircraft systems: air-ground channel characterization for future applications," *IEEE Vehicular Technology Magazine*, vol. 10, no. 2, pp. 79–85, 2015.

[24] W. Hapsari, "Study on enhanced LTE support for aerial vehicles, 3GPP," Sophia Antipolis, France, 2017, Rep. TR 36.777.

[25] J. Vince, *Mathematics for Computer Graphics*, Springer-Verlag, Heidelberg, 2009.

[26] R. M. Corless, G. H. Gonnet, D. E. G. Hare, D. J. Jeffrey, and D. E. Knuth, "On the LambertW function," *Advances in Computational Mathematics*, vol. 5, no. 1, pp. 329–359, 1996.